THE PUBLISHING HOUSE
OF THE ROMANIAN ACADEMY

PROCEEDINGS OF THE ROMANIAN ACADEMY, Series A,
Volume 23, Number 2/2022, pp. 143–152

MODELING OF A MAGNETO-ELECTRO-PIEZO-THERMOELASTIC NANOBEAM WITH TWO TEMPERATURE SUBJECTED TO RAMP TYPE HEATING

Iqbal KAUR[1], Kulvinder SINGH[2], Gilbert Marius Daniel GHITA[3], Eduard-Marius CRACIUN[4]

[1] Government College for Girls, Palwal Kurukshetra, Haryana, India, bawahanda@gmail.com
[2] Kurukshetra University, Kurukshetra, Haryana, India, ksingh2015@kuk.ac.in
[3] Ovidius University of Constanta, Romania, ghitamariusdan@yahoo.com
[4] Corresponding author: E.-M. Craciun, E-mail: mcraciun@univ-ovidius.ro

Abstract. In this research paper, a novel application of one-dimensional magneto-electro-piezo-thermoelastic (MEPT) Euler-Bernoulli nanobeam subjected to sinusoidally varying two temperature has been presented. Heat conduction equation with two temperature has been considered. The clamped-clamped architecture of the nanobeam has been considered in this study. One of the end is thermally insulated and the other end of the nanobeam is loaded with ramp-type heating. The derived mathematical model is used to find the dimensionless expressions for a thermal moment, lateral deflection, conductive temperature, axial stress, magnetic and electric potential. The effect of two temperature parameters, ramp parameter and initial electric potential on the electric potential, thermal moment, lateral deflection, axial stress and magnetic potential are investigated graphically.

Key words: magneto-electro-piezo-thermoelastic, nanobeam, two temperature, time harmonic frequency, electric and magnetic fields.

Nomenclature

Symbol	Nomenclature	SI Units
δ_{ij}	Kronecker delta	
w	Lateral deflection of the beam	m
t	Time	s
ϵ_{ijk}	Tensors of piezoelectric moduli measured at constant temperature	$\mathrm{C\,m^{-2}}$
t_{ij}	Stress tensors	$\mathrm{kg\,m^{-1}s^{-2}}$
u_i	Displacement components	m
E_i	Electric field	
E	Piezoelectric field flexure of the beam	
C_E	Specific heat	$\mathrm{J\,kg^{-1}K^{-1}}$
α_{ij}	Linear thermal expansion coefficient	$\mathrm{K^{-1}}$
ζ_{ij}	Tensors of dielectric moduli or permittivity constant at constant strain and constant temperature	$\mathrm{C\,V^{-1}m^{-1}}$
K_{ij}	Thermal conductivity	$\mathrm{W/(m\,K)}$
λ_i	Pyromagnetic coefficient	$\mathrm{C\,N^{-1}}$
$c_{11}I$	Flexural rigidity of the beam	$\mathrm{N\,m^2}$
B_i	Magnetic displacement	$\mathrm{A\,m^{-2}}$
γ	Magnetic potential	A
$\beta_1 M_T$	Thermal moment of the beam	
M	Flexural moment of the cross-section of a beam	$\mathrm{N\,m^{-2}}$
T_0	Reference temperature	K

e_{ij}	Strain tensors	
ϕ_0	Initial electric potential	V
I	moment of inertia of the cross-section	$\mathrm{kg\,m^2}$
β_{ij}	Thermal elastic coupling tensor measured at constant electric field	$\mathrm{N\,m^{-2}K^{-1}}$
D_i	Electric displacement	$\mathrm{C\,m^{-2}}$
d_{in}	Magnetoelectric material coefficients	$\mathrm{N\,s\,V^{-1}C^{-1}}$
T	Thermodynamic temperature	K
a_{ij}	Two Temperature parameter	K
F	Thermal field-induced flexural rigidity of a beam	$\mathrm{N\,m^2}$
p_i	Tensors of pyroelectric moduli measured at constant strain	$\mathrm{C\,m^{-2}K^{-1}}$
ρ	Medium density	$\mathrm{kg\,m^{-3}}$
χ_{im}	Magnetic permeability coefficients	$\mathrm{N\,A^{-1}m^{-1}K^{-1}}$
γ_0	Initial magnetic potential	A
ϕ	Electric potential	V
M_T	Thermal moment of inertia	$\mathrm{kg\,m^2}$
q_{ijn}	Piezomagnetic material coefficients	$\mathrm{N\,A^{-1}m^{-1}}$
H	Magnetic fields-induced flexural rigidity of a beam	$\mathrm{N\,m^2}$
φ	Conductive temperature	K
t_0	Ramp type parameter	s
c_{ijkl}	21 elastic constants	$\mathrm{N\,m^{-2}}$

1. INTRODUCTION

Piezoelectric materials yield electricity on the application of mechanical or thermal stresses and conversely on application of electric field produces deformation. There is an extensive group of resources that show this phenomenon to some extent, including natural quartz crystals, polycrystalline piezoceramic, semi-crystalline polyvinylidene polymer, wood and even bone. There has been a sustained increase in the past decade in the use of smart materials (MEPT) as micro and nano-materials structures due to their special properties like piezoelectric, piezomagnetic, Pyromagnetic and magnetoelectric etc. in which the elastic deformations may be induced directly by mechanical loading/temperature gradient or indirectly by an application of electric or magnetic field. Due to these novel coupling features of MEPT material systems, their use in sensors, actuators, and structural components of micro-electromechanical systems (MEMS) and magneto-piezoelectric systems is expected to continue to grow.

Many articles describe piezoelectric and related materials' basic theories of elasticity, but few are cited here. Ebrahimi and Barati [1] studied the thermo–piezoelectrically triggered nanobeam with the magnetic field. Arefi [2] analyzed the wave propagation using the nonlocal elasticity model in magneto-electroelastic nano-rod due to electric and magnetic potentials. Sadek and Abukhaled [3] discussed piezoelectric actuators for suppressing vibrations in beams due to heat. The nonlocal piezoelectric rod studied by Li and He [4] was characterized by a moving heat source. Huang and Kuo [5] developed a formula for identifying the elastic magnetic and electric fields of a composite due to piezo-electric and piezo-magnetic phases. Additionally, other researchers used other thermoelasticity theories to work on the nanobeams as Elaziz *et al.* [6], Singh *et al.* [7], Craciun *et al.* [8], Khisaeva and Ostoja-Starzewski [9], Singh *et al.* [10], Abbas [11], Lata and Kaur [12], Kaur *et al.* [13–16].

Presenting these novel features, one-dimensional MEPT clamped-clamped nanobeam has been studied with sinusoidal varying conductive temperature. One of the ends of the nanobeam is thermally insulated and the other end is loaded with ramp-type heating. The imbalance of temperature leads to deformation of nanobeam and hence yields electricity. The effect of two temperature, ramp parameter, initial electric potential, initial magnetic potential on electric potential, thermal moment, lateral deflection, axial stress and magnetic potential have been investigated graphically using the MATLAB software.

2. BASIC EQUATIONS

Following Ebrahimi and Barati [1] the constitutive relations, eq. of motion, gauss eq. and heat conduction eq. with two temperature, in the absence of heat sources, body forces and charge density, for an MEPT medium, are given by

i. Constitutive relations

$$t_{ij} = c_{ijkl}e_{kl} - \epsilon_{ijk}E_k - q_{ijn}H_n - \beta_{ij}T\,, \tag{1}$$

$$D_i = \zeta_{im}E_m + \epsilon_{ijk}e_{jk} + d_{in}H_n - p_iT\,; \quad B_i = \chi_{im}H_m + q_{ijk}e_{jk} + d_{in}E_n - \lambda_iT\,, \tag{2}$$

$$E_i = -\phi_{,i}\,, \quad H_i = -\gamma_{,i}\,, \tag{3}$$

where, $\beta_{ij} = c_{ijkl}\alpha_{kl}$, $T = \varphi - a_{ij}\varphi_{,ij}$, $e_{kl} = \frac{1}{2}\left(\frac{\partial u_k}{\partial x_l} + \frac{\partial u_l}{\partial x_k}\right)$, $(i, j, k, l = x, y, z)$.

ii. Equation of motion

$$t_{ij,j} = \rho\ddot{u}_i\,.$$

iii. Gauss equation

$$D_{i,i} = 0, \quad B_{i,i} = 0\,. \tag{4}$$

iv. Heat conduction equation

$$K_{ij}\varphi_{,ij} = \rho C_E\dot{T} + T_0\beta_{ij}\dot{u}_{i,j} - T_0p_i\dot{\phi}_{,i} - T_0\lambda_i\dot{\gamma}_{,i}\,. \tag{5}$$

The symmetric properties of material constants are, $c_{ijkl} = c_{klij} = c_{jikl} = c_{ijlk}$, $\epsilon_{ijk} = \epsilon_{ikj}$, $\zeta_{im} = \zeta_{mi}$, $\beta_{ij} = \beta_{ji}$. The commas trailed by suffixes signify material derivatives, and a superimposed dot signifies derivatives w.r.t. time.

3. FORMULATION OF THE PROBLEM

Consider the free vibrations of a homogeneous MEPT rectangular nanobeam with length $L\left(0 \le x \le L\right)$, width $b\left(-\frac{b}{2} \le y \le \frac{b}{2}\right)$ and thickness $h\left(-\frac{h}{2} \le z \le \frac{h}{2}\right)$, (where *x*, *y* and *z* are the cartesian axes, with the constant cross-sectional area). Axis of the nanobeam is *x*-axis, and one of the end of the nanobeam, the *y*–*z* plane ($x = 0$) with the origin at its centre. The nanobeam is initially unstrained, unstressed at a uniform temperature T_0. For the thin beam, both the transverse shear deformations, transverse shear strains and rotatory inertias can be neglected. Also, in-plane electric fields can be ignored i.e. $E_x = 0 = E_y$ and electric field (E_z) is considered in this study, and hence perpendicular component of magnetic field (H_x) exists and $H_z = 0 = H_y$. There are small bending vibrations of the beam about the *x*-axis s.t. the deflection is consistent with the linear Euler–Bernoulli theory [18], according to which "During bending, any plane cross-section initially parallel to the beam's axis remains parallel and perpendicular to the neutral surface". The displacement components of the Euler-Bernoulli theory for a simple deflection problem are given by Rao [18] as,

$$u(x,y,z,t) = -z\frac{\partial w}{\partial x},\quad v(x,y,z,t) = 0,\quad w(x,y,z,t) = w(x,t)\,. \tag{6}$$

Consider that along the thickness direction temperature is varying sinusoidally.

$$\varphi(x,z,t) = \theta(x,t)\sin\frac{\pi z}{h}\,. \tag{7}$$

Initially, the material lies at rest without any disturbance. As a result,

$$w(x,0) = 0,\quad \frac{\partial w}{\partial t}(x,0) = 0,\quad \varphi(x,z,0) = 0,\quad \frac{\partial \varphi}{\partial t}(x,z,0) = 0\,. \tag{8}$$

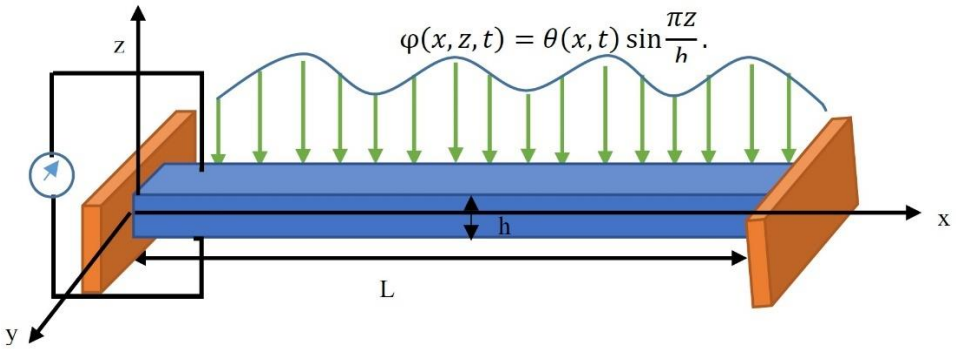

Fig. 1 – Schematic view of the nanobeam.

4. SOLUTION OF THE PROBLEM

With the help of eq. (3) and (6), the constitutive equation can be obtained from eqns. (1) and (2) as

$$t_{xx} = -c_{11}z\frac{\partial^2 w}{\partial x^2} - \epsilon_{31}\frac{\partial \phi}{\partial z} - \beta_1 T\,,\quad t_{zz} = -c_{13}z\frac{\partial^2 w}{\partial x^2} - \epsilon_{33}\frac{\partial \phi}{\partial z} - \beta_3 T\,, \tag{9}$$

$$D_x = -d_{11}\frac{\partial \gamma}{\partial x},\quad D_y = 0,\quad D_z = -\epsilon_{31}z\frac{\partial^2 w}{\partial x^2} - \zeta_{33}\frac{\partial \phi}{\partial z} + p_3 T\,, \tag{10}$$

$$B_x = -\chi_{11}\frac{\partial \gamma}{\partial x},\quad B_y = 0,\quad B_z = -q_{31}z\frac{\partial^2 w}{\partial x^2} - d_{33}\frac{\partial \phi}{\partial z} + \lambda_3 T\,. \tag{11}$$

Equation (4) with the help of eq. (10) and (11) takes the form

$$\epsilon_{31}\frac{\partial^2 w}{\partial x^2}+\zeta_{33}\frac{\partial^2 \phi}{\partial z^2}+d_{11}\frac{\partial^2 \gamma}{\partial x^2}=p_3\frac{\partial T}{\partial z} \tag{12a}$$

$$q_{31}\frac{\partial^2 w}{\partial x^2}+d_{33}\frac{\partial^2 \phi}{\partial z^2}+\chi_{11}\frac{\partial^2 \gamma}{\partial x^2}=\lambda_3\frac{\partial T}{\partial z}\,. \tag{12b}$$

Integrating (12a) and (12b) w.r.t. z and eliminating first γ from both equations and then eliminating ϕ gives

$$\frac{\partial \phi}{\partial z}=Az\frac{\partial^2 w}{\partial x^2}+BT+\phi_0\,;\quad \frac{\partial^2 \gamma}{\partial x^2}z=Cz\frac{\partial^2 w}{\partial x^2}+FT\,, \tag{13}$$

where, $A=\dfrac{\epsilon_{31}\chi_{11}-q_{31}d_{11}}{d_{33}d_{11}-\chi_{11}\zeta_{33}}$, $B=\dfrac{\lambda_3 d_{11}-p_3\chi_{11}}{d_{33}d_{11}-\chi_{11}\zeta_{33}}$, $C=\dfrac{q_{31}\zeta_{33}-\epsilon_{31}d_{33}}{d_{33}d_{11}-\chi_{11}\zeta_{33}}$, $F=\dfrac{p_3 d_{33}-\lambda_3\zeta_{33}}{d_{33}d_{11}-\chi_{11}\zeta_{33}}$.
Also supposing that $t_{zz}=0$, implies that

$$\beta_3 T=-c_{13}z\frac{\partial^2 w}{\partial x^2}-\epsilon_{33}\frac{\partial \phi}{\partial z}\,. \tag{14}$$

Eliminating T in first equations in (13) using (14) gives

$$\frac{\partial \phi}{\partial z}=\bar{c}_{13}z\frac{\partial^2 w}{\partial x^2}+\delta_1\,, \tag{15}$$

where, $\bar{c}_{13}=\dfrac{A\beta_3-c_{13}B}{B\epsilon_{33}+\beta_3}$, $\delta_1=\left(\dfrac{\phi_0\beta_3}{B\epsilon_{33}+\beta_3}\right)$. Integrating (15) w.r.t z (for limits $z=0$ to z) and considering the surfaces of the beam are electrically shorted (electrode surfaces) and hence $\phi=0$ at $z=\pm\dfrac{h}{2}$,

$$\phi(x,z,t)=\frac{\bar{c}_{13}}{2}\left(z^2-\frac{h^2}{4}\right)\frac{\partial^2 w}{\partial x^2}+\delta_1\left(z-\frac{h}{2}\right). \tag{16}$$

Following Rao [18], the flexural moment of a nanobeams cross-section is as follows

$$M(x,t)=-\int_{\frac{-h}{2}}^{\frac{h}{2}}\int_{\frac{-b}{2}}^{\frac{b}{2}} t_{xx}\,z\,\mathrm{d}z\mathrm{d}y=\bar{c}_{11}I\frac{\partial^2 w}{\partial x^2}+GM_T=\bar{c}_{11}I\frac{\partial^2 w}{\partial x^2}+G\int_{\frac{-h}{2}}^{\frac{h}{2}}T\,z\,\mathrm{d}z\,, \tag{17}$$

where $\bar{c}_{11}=-c_{11}-A\epsilon_{31}$, $I=\dfrac{bh^3}{12}$, $G=-b\left(\epsilon_{31}B+\beta_1\right)$. The transverse deflection of the nanobeam with free vibrations is

$$\frac{\partial^2 M}{\partial x^2}+\rho A\frac{\partial^2 w}{\partial t^2}=0\,, \tag{18}$$

where A(area of cross-section) $=bh$. Equation (18) when applied to equation (17) yields

$$D^*\frac{\partial^4 w}{\partial x^4}+G\frac{\partial^2 M_T}{\partial x^2}+\rho A\frac{\partial^2 w}{\partial t^2}=0\,, \tag{19}$$

where $D^*=\bar{c}_{11}I$. The equation (5) when $\varphi=\varphi(x,z,t)$ and using (9), (16) can be written as

$$K_1\frac{\partial^2 \varphi}{\partial x^2}+K_3\frac{\partial^2 \varphi}{\partial z^2}=T_0 b_1^*\frac{\partial}{\partial t}\left(z\frac{\partial^2 w}{\partial x^2}\right)+\rho C_E\frac{\partial T}{\partial t}\,, \tag{20}$$

where $b_1^* = -(\beta_1 + p_3\bar{c}_{13})$. To solve this problem the dimensionless quantities are given by:

$$\begin{gathered}(x', z', w', h', b', \phi', \gamma', \delta') = \frac{1}{L}(x, z, w, h, b, \phi, \gamma, \delta),\ (t', t_0', t_1') = \frac{c_1}{L}(t, t_0, t_1),\ (T', \varphi') = \frac{1}{T_0}(T, \varphi),\\ \rho c_1^2 = c_{11},\ t_{xx}' = \frac{t_{xx}}{\beta_1 T_0},\ M_T' = \frac{M_T}{T_0 L^3},\ (a_1', a_3') = \frac{1}{L^2}(a_1, a_3),\ q' = \frac{q}{L},\ Q' = \frac{L^2 Q}{K_1 T_0},\ b_1^{*'} = L b_1^*.\end{gathered} \tag{21}$$

Laplace transforms is defined by

$$\bar{f}(x, z, s) = \int_0^\infty f(x, z, t)\, \mathrm{e}^{-st}\, \mathrm{d}t\,. \tag{22}$$

Apply dimensionless quantities (21) on the eq. (7), (16), (19) and (20) and after suppressing the prime and then apply Laplace transform (22) the non-dimensional form of the equations we have

$$\bar{\varphi}(x, z, s) = \bar{\theta}(x, s) \sin\frac{\pi z}{h}, \tag{23}$$

$$\bar{\phi}(x, z, s) = \frac{\bar{c}_{13}}{2}\left(z^2 - \frac{h^2}{4}\right)\frac{\mathrm{d}^2\bar{w}}{\mathrm{d}x^2} + \delta_1\left(z - \frac{h}{2}\right), \tag{24}$$

$$D^* \frac{\mathrm{d}^4\bar{w}}{\mathrm{d}x^4} + \eta_4 \frac{\mathrm{d}^2\overline{M_T}}{\mathrm{d}x^2} + \eta_5\bar{w} = 0\,, \tag{25}$$

$$\eta_6 \frac{\partial^2\bar{\varphi}}{\partial x^2} + \frac{\partial^2\bar{\varphi}}{\partial z^2} - \eta_7\bar{\varphi} = \eta_8\left(z\frac{\mathrm{d}^2\bar{w}}{\mathrm{d}x^2}\right), \tag{26}$$

where, $\eta_1 = \frac{K_3}{K_1},\ \eta_2 = \frac{\rho C_E L s}{K_1},\ \eta_3 = \frac{b_1^* s}{K_1},\ \eta_4 = GT_0 L,\ \eta_5 = c_{11}s^2,\ \eta_6 = \frac{(1+\eta_2 a_1)}{(\eta_1 + \eta_2 a_3)},\ \eta_7 = \frac{\eta_2}{(\eta_1 + \eta_2 a_3)},$ $\eta_8 = \frac{\eta_3}{(\eta_1 + \eta_2 a_3)}$. Using eq. (23) in (25) for $\overline{M_T}$, we get eq. (27) and using eq. (23) in (26) and after multiplying by z and integrating with respect to *z* for limits $\left(-\frac{h}{2} \le z \le \frac{h}{2}\right)$ we get eq. (28) as

$$\left(D^* D^4 + \eta_5\right)\bar{w} + \left[\eta_9 D^2 - \eta_{10} D^4\right]\bar{\theta} = 0\,, \tag{27}$$

$$\eta_{12} D^2\bar{w} - \left(\eta_6 D^2 - \eta_{11}\right)\bar{\theta} = 0\,, \tag{28}$$

where $\eta_9 = \eta_4\left(\frac{2h^2}{\pi^2} + 2a_3\right),\ \eta_{10} = a_1\frac{2h^2}{\pi^2}\eta_4,\ \eta_{11} = \eta_7 - \frac{\pi^2}{h^2},\ \eta_{12} = \eta_8\frac{\pi^2}{24},\ D \equiv \frac{\mathrm{d}}{\mathrm{d}x}$. From equations (27) and (28), we get

$$\left[D^6 - pD^4 + qD^2 - r\right]\left(\bar{w}, \bar{\Theta}\right)(x, s) = 0\,, \tag{29}$$

where, $p = \frac{\eta_{12}\eta_{10} + \eta_{11}D^*}{\eta_6 D^*},\ q = \frac{\eta_{12}\eta_9 + \eta_5\eta_6}{\eta_6 D^*},\ r = \frac{\eta_5\eta_{11}}{\eta_6 D^*}$. The differential equation governing the lateral deflection $\bar{w}(x, s)$, equation (29) is a bicubic equation can takes form

$$\left(D^2 - \lambda_1^2\right)\left(D^2 - \lambda_2^2\right)\left(D^2 - \lambda_3^2\right)\left(\bar{w}, \bar{\Theta}\right)(x, s) = 0\,, \tag{30}$$

where $\pm\lambda_1, \pm\lambda_2$ and $\pm\lambda_3$ are the characteristics roots of the equation $\lambda^6 - p\lambda^4 + q\lambda^2 - r = 0$ and hence lateral displacement becomes

$$\bar{w}(x,s) = \sum_{i=1}^{3}\left[A_i(s)\mathrm{e}^{-\lambda_i x} + A_{i+3}(s)\mathrm{e}^{\lambda_i x}\right]. \tag{31}$$

Using $\bar{w}(x,s)$ from eq. (31) in eq. (28) we obtain eq. (32) and then using $\bar{\Theta}(x,s)$ from eq. (32) in eq. (23) we obtain conductive temperature given in eq. (33) and hence thermal moment in eq. (34)

$$\bar{\Theta}(x,s) = \sum_{i=1}^{3}\varrho_i\left[A_i\mathrm{e}^{-\lambda_i x} + A_{i+3}\mathrm{e}^{\lambda_i x}\right], \tag{32}$$

$$\bar{\varphi}(x,z,s) = \left\{\sum_{i=1}^{3}\varrho_i\left[A_i\mathrm{e}^{-\lambda_i x} + A_{i+3}\mathrm{e}^{\lambda_i x}\right]\right\}\sin\frac{\pi z}{h}, \tag{33}$$

$$\bar{M}_T(x,s) = \sum_{i=1}^{3}C_i\left[A_i\mathrm{e}^{-\lambda_i x} + A_{i+3}\mathrm{e}^{\lambda_i x}\right], \tag{34}$$

where, $\varrho_i = \left(\dfrac{\eta_{12}\lambda_i^2}{\eta_6\lambda_i^2 - \eta_{11}}\right)$, $i = 1,2,3$; $C_i = \left[\dfrac{2bh^2}{\pi^2}\left(1 - a_1\lambda_i^2\right) + 2ba_3\right]\varrho_i$, $i = 1,2,3$.

Thus using (31) and (32) in (16) we obtain electric potential, magnetic potential and axial stress $\bar{t}_{xx}(x,z,s)$ as

$$\phi(x,z,s) = \frac{\bar{c}_{13}}{2}\left(z^2 - \frac{h^2}{4}\right)\sum_{i=1}^{3}\lambda_i^2\left[A_i(s)\mathrm{e}^{-\lambda_i x} + A_{i+3}(s)\mathrm{e}^{\lambda_i x}\right] + \delta_4\left(z - \frac{h}{2}\right), \tag{35}$$

$$\gamma(x,z,s) = \sum_{i=1}^{3}\left[A_i\mathrm{e}^{-\lambda_i x} + A_{i+3}\mathrm{e}^{\lambda_i x}\right]L_i, \tag{36}$$

$$\bar{t}_{xx}(x,z,s) = \sum_{i=1}^{3}G_i\left[A_i\mathrm{e}^{-\lambda_i x} + A_{i+3}\mathrm{e}^{\lambda_i x}\right], \tag{37}$$

where $G_i = \left\{-c_{11}z\lambda_i^2 + \epsilon_{31}\left(\bar{c}_{13}\lambda_i^2 z + \delta_4\right) + q_{31}\left(\bar{\bar{c}}_{13}\lambda_i^2 z + \delta_5\right) - \varrho_i\beta_1\sin\dfrac{\pi z}{h}\left[\left(1 + a_3\dfrac{\pi^2}{h^2}\right) - a_1\lambda_i^2\right]\right\}$,

$L_i = 1 + \dfrac{F\sin\dfrac{\pi z}{h}}{z\lambda_i^2}\varrho_i\left(1 - a_1\lambda_i^2 + a_3\dfrac{\pi^2}{h^2}\right)$ $\left(\text{assuming } \gamma = \dfrac{\partial\gamma}{\partial x} = 0 \text{ at } x = 0\right)$.

5. BOUNDARY CONDITIONS

1. For clamped-clamped architecture of the nanobeam the boundary conditions [19] can be written as:

$$w(0,t) = 0, \quad w(L,t) = 0, \quad \frac{\partial w}{\partial x}(0,t) = 0, \quad \frac{\partial w}{\partial x}(L,t) = 0. \tag{38}$$

2. Consider that the end $x = 0$ of the nanoscale beam is thermally loaded by ramp type heating, and the other end $x = L$, is thermally insulated

$$\varphi(0,z,t) = \varphi_1(z)\times\begin{cases} 0, & t = 0, \\ \dfrac{t}{t_0}, & 0 < t < t_0, \text{ and } \dfrac{\partial\varphi}{\partial x}(L,z,t) = 0, \\ 1, & t = t_0. \end{cases} \tag{39}$$

Thus applying dimensionless quantities on (38)–(39) and then taking their Laplace transform we have

$$w(0,s)=w(1,s)=\frac{\partial w}{\partial x}(0,s)=\frac{\partial w}{\partial x}(1,s)=0,\ \ \varphi(0,z,s)=\varphi_1(z)\Gamma_1',\ \ \frac{\partial \varphi}{\partial x}(1,z,s)=0\,, \tag{40}$$

where, $\Gamma_1'=\dfrac{1-\mathrm{e}^{-st_0}}{s^2t_0}$, $\varphi_1(z)=\sin\dfrac{\pi z}{h}$. Solving (40), we obtain the value of A_i as

$$A_i=\frac{\Delta_i}{\Delta}\ ,\ \ i=1,2,3,\ldots,6 \tag{41}$$

$$\Delta=\begin{vmatrix} 1 & 1 & 1 & 1 & 1 & 1 \\ -\lambda_1 & -\lambda_2 & -\lambda_3 & \lambda_1 & \lambda_2 & \lambda_3 \\ e^{-\lambda_1} & e^{-\lambda_2} & e^{-\lambda_3} & e^{\lambda_1} & e^{\lambda_2} & e^{\lambda_3} \\ -\lambda_1 e^{-\lambda_1} & -\lambda_2 e^{-\lambda_2} & -\lambda_3 e^{-\lambda_3} & \lambda_1 e^{\lambda_1} & \lambda_2 e^{\lambda_2} & \lambda_3 e^{\lambda_3} \\ \varrho_1 & \varrho_2 & \varrho_3 & \varrho_1 & \varrho_2 & \varrho_3 \\ -\lambda_1\varrho_1 e^{-\lambda_1} & -\lambda_2\varrho_2 e^{-\lambda_2} & -\lambda_3\varrho_3 e^{-\lambda_3} & \lambda_1\varrho_1 e^{\lambda_1} & \lambda_2\varrho_2 e^{\lambda_2} & \lambda_3\varrho_3 e^{\lambda_3} \end{vmatrix},$$

where $\Delta_i\,(i=1,2,3,\ldots,6)$ are found by substituting the columns by $\begin{bmatrix}0 & 0 & 0 & 0 & \Gamma_1' & 0\end{bmatrix}'$ in Δ.

6. INVERSION OF LAPLACE TRANSFORM

To obtain the function $f(x,t)$ of eqns. (31)–(41) in the physical domain, invert the Laplace transform by

$$f(x,t)=\frac{1}{2\pi i}\int_{\mathrm{e}^{-i\infty}}^{\mathrm{e}^{+i\infty}}\bar{f}(x,s)\mathrm{e}^{-st}\mathrm{d}s\,. \tag{42}$$

A description of how to calculate this integral can be found in Press et al. [20], *"which uses Romberg's integration with adaptive step size. This also uses the results from successive refinements of the extended trapezoidal rule followed by extrapolation of the results to the limit when the step size tends to zero"*.

7. RESULTS AND DISCUSSION

The influence of frequency, initial electric potential and initial magnetic potential in the theoretical results is proved for MEPT material $BaTiO_3$-$CuFe_2O_4$, and the physical data following Ansari and Gholami [21] is:

$$c_{11}=226\,\mathrm{GPa},\ p_3=25\times10^6\,\mathrm{C\,m^{-2}K^{-1}},\ \lambda_3=5.19\times10^6\,\mathrm{CN^{-1}},\ \chi_{33}=83.5\times10^6\,\mathrm{NA^{-1}m^{-1}K^{-1}},\ c_{13}=124\,\mathrm{GPa}\,,$$

$$\epsilon_{31}=2.2\,\mathrm{C\,m^{-2}},\ d_{33}=2737.5\times10^{12}\,\mathrm{Ns\,V^{-1}C^{-1}},\ q_{31}=290.1\,\mathrm{NA^{-1}m^{-1}},\ \zeta_{33}=6.35\times10^9\,\mathrm{CV^{-1}m^{-1}},\ C_E=420\,\mathrm{J\,kg^{-1}K^{-1}},$$

$$L/h=10,\ \ b/h=0.5,\ \ \beta_1=4.74\times10^5\,\mathrm{Nm^{-2}K^{-1}},\ \ \beta_3=4.53\times10^5\,\mathrm{Nm^{-2}K^{-1}},\ \ K_1=1.53\times10^2\,\mathrm{Wm^{-1}K^{-1}},$$

$$K_3=1.53\,\mathrm{Wm^{-1}K^{-1}},\ \ \rho=7.75\times10^3\,\mathrm{kg\,m^{-3}},\ \ t_0=0.20\,\mathrm{ps}\,.$$

Figure 2 exhibits the dissemination of electric potential with *x* for various values of two temperatures. It is observed that without two temperatures, there is a sharp increase in the electric potential. Moreover, it is seen that a_1 has the more effect as compared to a_3. Figure 3 illustrates the variation in magnetic potential with *x* for different values of two temperatures. It is observed that without two temperatures, there is a sharp variation in the magnetic potential. Moreover, it is seen that a_1 has the more effect on magnetic potential as compared to a_3. Figure 4 shows the dissemination of electric potential with *x* for various values of initial electric potential. It is perceived that the electric potential sharply rises with the increases with the initial electrical potential. The higher the initial electric potential, higher will be the variation in the distribution of electric potential. Figure 5 exhibits the magnetic potential with *x* for different values of ramp parameter. It is seen that

the magnetic potential sharply drops with the increases in *x*, but the higher the preliminary electric potential, higher will be the variation in the distribution of magnetic potential. Figure 6 illustrates the deviation of Electric Potential with *x* for various values of *z*. It is found that the electric potential has the same values for $z = \mp\frac{h}{2}$. moreover, for further values of *z*.

Figure 7 exhibits the deviation in magnetic potential with *x* for various values of *z*. It is found that the magnetic potential has the same values for $z = \mp\frac{h}{2}$. However, magnetic potential shows the maximum variation for $z = \mp\frac{h}{4}$.

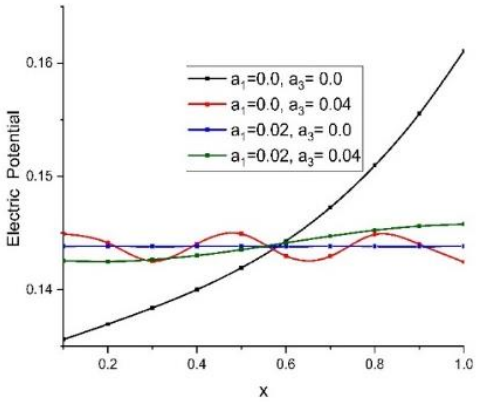

Fig. 2 – Deviation of electric potential for various values of two temperatures.

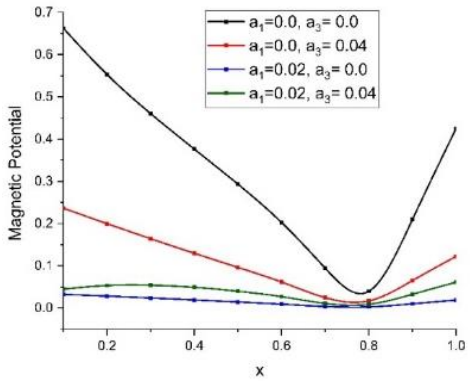

Fig. 3 – Deviation of magnetic potential for various values of two temperatures.

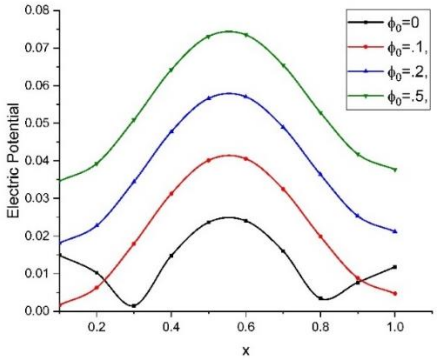

Fig. 4 – Deviation of electric potential for various values of initial electric potential.

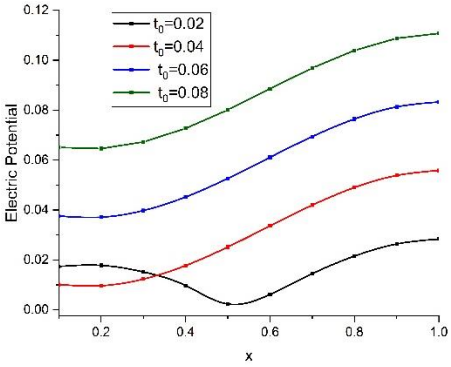

Fig. 5 – Deviation of electric potential for various values of ramp parameter.

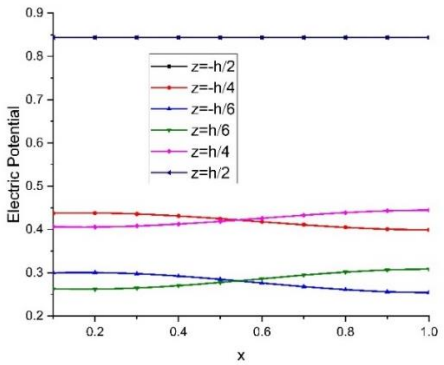

Fig. 6 – Deviation of electric potential for various values of *z*.

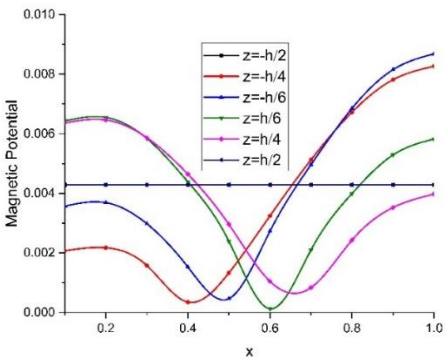

Fig. 7 – Deviation of magnetic potential for various values of *z*.

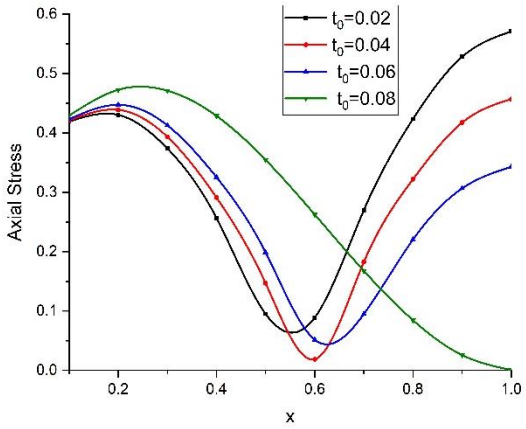

Fig. 8 – Deviation of axial stress for various values of ramp parameter

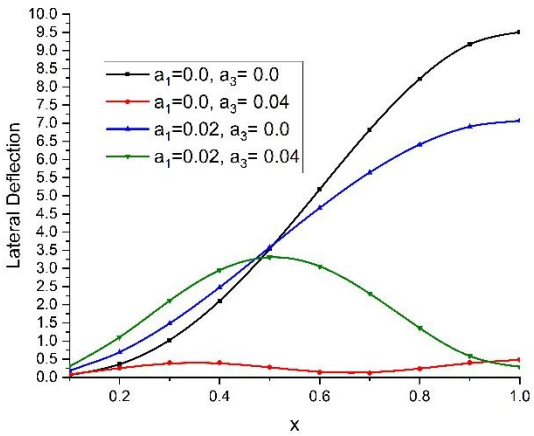

Fig. 9 – Deviation of lateral deflection for various values of two temperature parameter

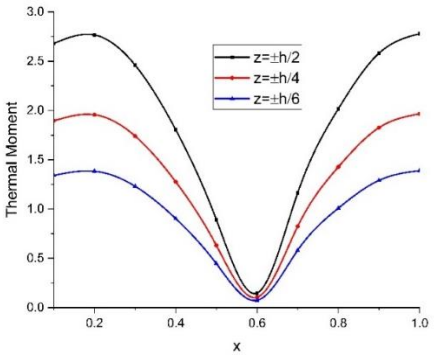

Fig. 10 – Deviation of the thermal moment for various values of *z*.

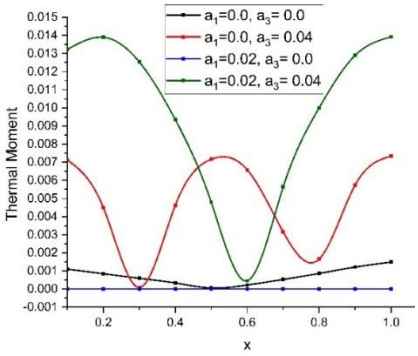

Fig. 11 – Deviation of the thermal moment for various values of two temperatures.

Figure 8 illustrates the distribution of axial stress with *x* for various values of ramp parameter. It is seen that for Higher the ramp parameter, higher will be the variation in the distribution of axial stress.

Figure 9 illustrates the distribution of lateral deflection with *x* for various values of two temperature parameter. It is found that with increase in two temperature parameter, lateral deflection is lowered.

Figure 10 shows the variation in the thermal moment with *x* for various values of *z*. It is seen that the thermal moment has the same values for $z = \mp\frac{h}{2}, \mp\frac{h}{4}$ and $\mp\frac{h}{6}$.

Figure 11 shows the variation in the thermal moment with *x* for various values of two temperatures. It is seen that a_1 has the more effect as compared to a_3.

8. CONCLUSIONS

- Based on the mathematical model of Euler Bernoulli beams, the MEPT clamped-clamped nanobeams, subjected to electric and magnetic potentials are analysed in this study.
- We obtained the dimensionless expressions for electric potential, thermal moment, lateral deflection, magnetic potential, conductive temperature, and axial stress.
- The effect of two temperatures on the electric potential, lateral deflection, thermal moment and magnetic potential are characterized explicitly. The results show that a_1 has the more effect as compared to a_3. However, electric potential, thermal moment, lateral deflection and magnetic potential show dissimilar behaviour with different values of the two temperatures.
- In addition, the effect of *z* on the thermal moment, electric and magnetic potential is characterized graphically. It is observed that higher is the initial electric potential, initial magnetic potential, higher is the variation in parameters. However, these parameters depict the same values for $z = \mp\frac{h}{2}, \mp\frac{h}{4}$ and $\mp\frac{h}{6}$.

• Comparisons are made with different values of ramp parameter on magnetic potential and axial stress on the nanobeam and variation of initial electric potential on electric potential. It is observed that higher is the initial electric potential, higher is the variation in electric potential.

• As an application, this study helps in designing the sensing, actuation, and NEMS/ MEMS-based devices for marine and aerospace industries, energy harvesting, navigation, and sonar projectors. etc.

REFERENCES

1. F. EBRAHIMI, M.R. BARATI, *Dynamic modeling of a thermo–piezo-electrically actuated nanosize beam subjected to a magnetic field*, Appl. Phys. A, **122**, *4*, art. 451, 2016, doi: 10.1007/s00339-016-0001-3.
2. M. AREFI, *Analysis of wave in a functionally graded magneto-electro-elastic nano-rod using nonlocal elasticity model subjected to electric and magnetic potentials*, Acta Mech., **227**, *9*, pp. 2529–2542, 2016, doi: 10.1007/s00707-016-1584-7.
3. I. SADEK, M. ABUKHALED, *Optimal control of thermoelastic beam vibrations by piezoelectric actuation*, J. Control Theory Appl., **11**, *3*, pp. 463–467, 2013, doi: 10.1007/s11768-013-1204-1.
4. D. LI, T. HE, *Investigation of generalized piezoelectric-thermoelastic problem with nonlocal effect and temperature-dependent properties*, Heliyon, **4**, *10*, art. e00860, 2018, doi: 10.1016/j.heliyon.2018.e00860.
5. J.H. HUANG, W.-S. KUO, *The analysis of piezoelectric/piezomagnetic composite materials containing ellipsoidal inclusions*, J. Appl. Phys., **81**, *3*, pp. 1378–1386, 1997, doi: 10.1063/1.363874.
6. E.M. ABD-ELAZIZ, M.I.A. OTHMAN, *Effect of Thomson and thermal loading due to laser pulse in a magneto-thermo-elastic porous medium with energy dissipation*, ZAMM - J. Appl. Math. Mech. / Zeitschrift für Angew. Math. und Mech., **99**, *8*, 2019, doi: 10.1002/zamm.201900079.
7. A. SINGH, S. DAS, E.-M. CRACIUN, *Effect of thermomechanical loading on an edge crack of finite length in an infinite orthotropic strip*, Mech. Compos. Mater., **55**, *3*, pp. 285–296, 2019, doi: 10.1007/s11029-019-09812-1.
8. E.-M. CRACIUN, E. BAESU, E. SOÓS, *General solution in terms of complex potentials for incremental antiplane states in prestressed and prepolarized piezoelectric crystals: application to Mode III fracture propagation*, IMA J. Appl. Math., **70**, *1*, pp. 39–52, 2004, doi: 10.1093/imamat/hxh060.
9. Z.F. KHISAEVA, M. OSTOJA-STARZEWSKI, *Thermoelastic damping in nanomechanical resonators with finite wave speeds*, J. Therm. Stress., **29**, *3*, pp. 201–216, 2006, doi: 10.1080/01495730500257490.
10. A. SINGH, S. DAS, H. ALTENBACH, E. -M. CRACIUN, *Semi-infinite moving crack in an orthotropic strip sandwiched between two identical half planes*, ZAMM - J. Appl. Math. Mech. / Zeitschrift für Angew. Math. und Mech., **100**, *2*, 2020, doi: 10.1002/zamm.201900202.
11. I.A. ABBAS, *Free vibrations of nanoscale beam under two-temperature Green and Naghdi model*, Int. J. Acoust. Vib., **23**, *3*, 2018, pp. 289–293, doi: 10.20855/ijav.2018.23.31051.
12. P. LATA, I. KAUR, *A study of transversely isotropic thermoelastic beam with Green-Naghdi Type-II and Type-III theories of thermoelasticity*, Appl. Appl. Math. An Int. J., **14**, *1*, pp. 270–283, 2019.
13. I. KAUR, P. LATA, K. SINGH, *Effect of Hall current in transversely isotropic magneto-thermoelastic rotating medium with fractional-order generalized heat transfer due to ramp-type heat*, Indian J. Phys., **95**, pp. 1165–1174, 2021, doi: 10.1007/s12648-020-01718-2.
14. I. KAUR, P. LATA, K. SINGH, *Study of transversely isotropic nonlocal thermoelastic thin nano-beam resonators with multi-dual-phase-lag theory*, Arch. Appl. Mech., **91**, *1*, pp. 317–341, 2021, doi: 10.1007/s00419-020-01771-7.
15. I. KAUR, P. LATA, K. SINGH, *Study of frequency shift and thermoelastic damping in transversely isotropic nano-beam with GN III theory and two temperature*, Arch. Appl. Mech., **91**, *4*, pp. 1697–1711, 2021, doi: 10.1007/s00419-020-01848-3.
16. I. KAUR, K. SINGH, G.M.D. GHITA, *New analytical method for dynamic response of thermoelastic damping in simply supported generalized piezothermoelastic nanobeam*, ZAMM - J. Appl. Math. Mech. / Zeitschrift für Angew. Math. und Mech., **101**, *10*, 2021, doi: 10.1002/zamm.202100108.
17. I. KAUR, P. LATA, *Axisymmetric deformation in transversely isotropic magneto-thermoelastic solid with Green–Naghdi III due to inclined load*, Int. J. Mech. Mater. Eng., **15**, *1*, 2020, doi: 10.1186/s40712-019-0111-8.
18. S.S. RAO, *Vibration of continuous systems*, John Wiley & Sons, New Jersey, 2007.
19. M. BAO, *Analysis and design principles of MEMS devices*, Elsevier Science, 2005.
20. William H. PRESS, Saul A. TEUKOLSKY, Brian P. FLANNERY, *Numerical recipes in Fortran*, Cambridge University Press, 1980.
21. R. ANSARI, R. GHOLAMI, *Nonlocal nonlinear first-order shear deformable beam model for postbuckling analysis of magneto-electro-thermo elastic nanobeams*, Sci. Iran., **23**, *6*, pp. 3099–3114, 2016, doi: 10.24200/sci.2016.4015.

Received May 11, 2021